

CCII-Based Linear Ratiometric Capacitive Sensing by Analog Read-Out Circuits

G. Ferri¹(✉), F.R. Parente¹, V. Stornelli¹, G. Barile¹, G. Pennazza²,
and M. Santonico²

¹ Department of Industrial and Information Engineering and Economics,
University of L'Aquila, L'Aquila, Italy
giuseppe.ferri@univaq.it

² University Campus Bio-Medico di Roma, Rome, Italy

Abstract. Two electronic interfaces performing a differential (or ratiometric) sensor capacitance to voltage conversion are here presented. The output signal is proportional to the measurand variation x . The two read-out circuits differ themselves in their input stage: the first has an input current-to-voltage conversion, while the second one employs an input voltage source. Both of the solutions utilize commercial second generation current conveyors (CCIIs) as active blocks, in particular AD844. Theoretical analysis, simulated and experimental results have shown a good accuracy. Considering a capacitance variation due to the relative distance change, interface sensitivity (S) and resolution (res) values are constant and satisfactory: for the first solution, $S = 8.54 \text{ V}/\mu\text{m}$ and $res = 674 \text{ pm}$ (capacitance resolution value is 89.85 fF , that is -79 dB), while, for the second one, $S = 8.13 \text{ V}/\mu\text{m}$ and $res = 814 \text{ pm}$ (capacitance resolution value is 108.5 fF , that is -77 dB).

Keywords: Differential capacitive sensor · CCII · Current mode · Analog front-end

1 Introduction

Capacitive sensors are solid-state devices that reveal and quantify variations of physical, chemical or biological parameters the change of a capacitor. They are typically formed by two metal parallel plates separated by an insulator layer [1] and can be employed in applications as accelerometers [2], position sensors [3], pressure sensors [4] etc., where capacitance values can range from less than 1 pF up to hundreds of pF or even to nF . Their interfaces are based on the conversion of the capacitive value and variation into a voltage, a frequency (or period), a phase, etc. [5–7].

Differential (or ratiometric) sensors are a sub-set of these capacitive sensors employed to reduce resolution problems related to low capacitive variations and common mode disturbs. They have suitable applications in hair flow motion, accelerometers, position or rotation detection, force, etc. Figure 1 shows a simple schematization of a ratiometric capacitive sensor consisting in a three plates capacitive system with two fixed plates. The simplest differential sensing element is the capacitive

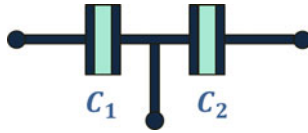


Fig. 1 Differential capacitance sensor structure

AC half-bridge where two capacitors change their value in a complementary way under a stimulus; unfortunately, this topology shows a reduced and not constant sensitivity.

In the literature, some analog interfaces for the ratiometric capacitive sensing have been proposed, based mainly on operational amplifiers [7–11], while current-mode interfaces are typically related to other sensor interfaces [12–17]. In this paper we propose two current conveyor-based interfaces performing a capacitive-to-voltage conversion, showing good and constant values of sensitivity and resolution.

2 The Current-Mode Interfaces

Considering Fig. 1, if the distance between the electrodes is changing, C_1 and C_2 have the following variations:

$$C_{1,2} = \frac{C_0}{2} \frac{1}{(1 \mp x)} \tag{1}$$

being C_0 the total capacitance of the transducer [9], from which measurand x can be expressed as independent from C_0 value as follows:

$$x = \frac{C_1 - C_2}{C_1 + C_2} \tag{2}$$

Figure 2 shows the first proposed interface (employing a current source as input signal), based on second generation current-conveyors (CCIIs).

From the properties of the ideal CCII ($V_X = V_Y$, $I_X = I_Z$ for the CCII+ and $I_X = -I_Z$ for the CCII-) [12], a straightforward analysis gives:

$$V_{out,pp}(x) = R'_L I_{IN,pp} \cdot \left[\frac{C_o}{C_o + C_3} x + \frac{C_3}{C_o + C_3} \right] \tag{3}$$

being R'_L the parallel impedance between the load resistance R_L (see Fig. 2) and the impedance parasitic component at CCII Z node at working frequency (R_Z) and $I_{IN,pp}$ the peak-to-peak value of the input current.

The second interface here proposed (Fig. 3) shows an input stage employing a CCII-based voltage-to-current converter [12]; in this manner, the voltage input signal can be more easily injected through a standard laboratory waveform generator.

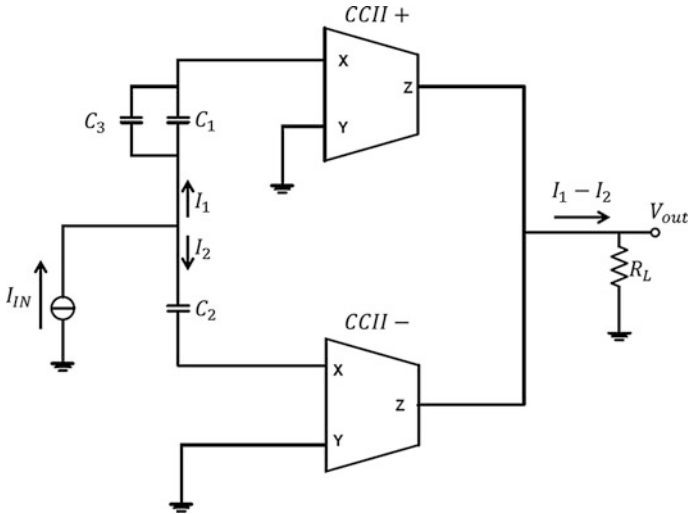


Fig. 2 The first proposed interface (C_1 and C_2 form the differential capacitive sensors)

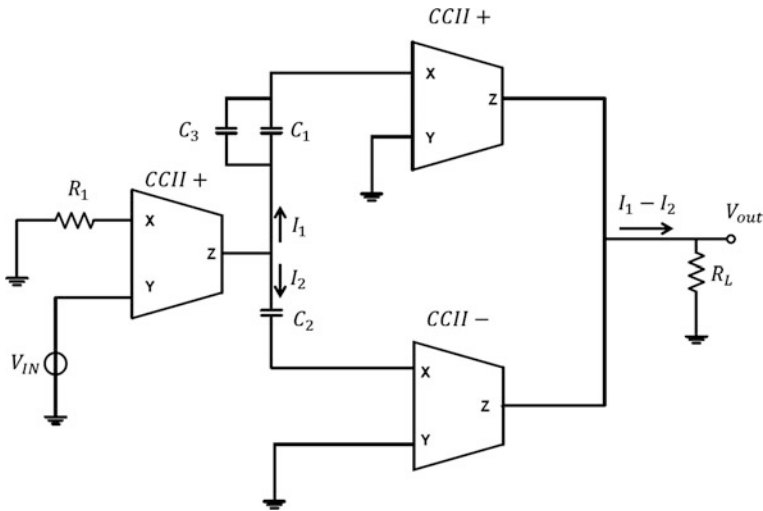


Fig. 3 The second proposed interface (C_1 and C_2 form the differential capacitive sensors) including the voltage to current converter as input stage

In this case, Eq. (3) becomes:

$$V_{out,pp}(x) = R'_L \frac{V_{IN,pp}}{R'_1} \cdot \left[\frac{C_o}{C_o + C_3} x + \frac{C_3}{C_o + C_3} \right] \tag{4}$$

being R'_L the parallel impedance between the load resistance R_L and the impedance parasitic component at CCII Z node at working frequency (R_Z), R'_1 the series

impedance between the resistance R_1 and the impedance parasitic component at CCII X node at working frequency (R_X) and $V_{IN,PP}$ the peak-to-peak value of the input voltage.

3 Results

For experimental measurements we have employed AD844 component as CCII+, while CCII- is implemented through a cascade of two AD844 devices [12]. The following nominal values have been considered: working frequency = 10 kHz and $R_L = 60 \text{ k}\Omega$; concerning the input signal amplitude, we chose $I_{IN,PP} = 1 \text{ mA}$ for the first interface and $V_{IN,PP} = 1 \text{ V}$, $R_1 = 1 \text{ k}\Omega$ for the second one. Furthermore, having considered AD844 parasitic components at the working frequency ($R_X = 50 \text{ }\Omega$, $R_Z = 3 \text{ M}\Omega$), we have obtained $R_1' = 1.05 \text{ k}\Omega$ and $R_L' = 57.629 \text{ k}\Omega$. We have considered a ratiometric capacitance sensing application, having a base-line value C_O of 800 pF and a 10% maximum relative variation (x). The transducer behavior has been emulated, in the experimental phase, by two capacitors. The value of C_3 has been set to 100 pF.

Starting from parallel plate capacitor model, we considered a possible capacitive variation related to a change in the initial distance between the capacitor plates, d_o :

$$C_{1,2} = \frac{\epsilon A}{(d_0 \mp \Delta d)} \tag{5}$$

The ratiometric equation becomes:

$$x = \frac{C_1 - C_2}{C_1 + C_2} = \frac{\Delta d}{d_0} \tag{6}$$

Concerning the first solution (shown in Fig. 2), we have performed only simulations that have been compared with the theory. Figure 4 shows the theoretical and

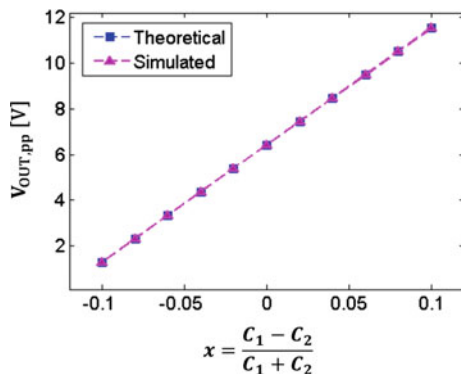


Fig. 4 First interface: output voltage (theoretical, simulated) versus x

simulated output voltages versus x parameter. The output range has been optimized, for the considered x variation, in the most part of the supply range. The relative percentage error is always lower, in absolute value, than 0.1%, so the proposed interface shows a good accuracy.

Having considered a MEMS application ($d_0 = 3 \mu\text{m}$), the sensitivity is constant and valued about $S = 8.54 \text{ V}/\mu\text{m}$. Sensitivity definition has been expressed according to [17]. Having evaluated a 576 nV output voltage noise, we have a resolution in terms of distance variation of about 674 pm, i.e., as capacitive value, of 89.85 fF (that is about -79 dB).

Concerning the second solution (Fig. 3), Fig. 5 shows the output voltage versus the measurand x . Theoretical, simulated (through Orcad-Spice software) and experimental results (averaged on 10 different measurements) are in a good agreement. Uncertainty on the experimental data has been expressed through the standard deviation: it is lower than 0.025 for the whole measurements. The relative percentage error has been calculated for the averaged experimental data is lower than 0.2% between simulations and theory and than 3% between theory and measurements.

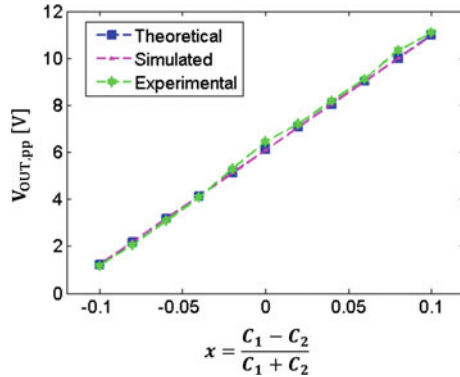


Fig. 5 Second interface: output voltage (theoretical, simulated, measured) versus x

Then, having considered $d_0 = 3 \mu\text{m}$, sensitivity value for the second interface is constant and valued about $8.13 \text{ V}/\mu\text{m}$. Having evaluated a 662 nV output voltage noise, we have a resolution of about 814 pm for the above mentioned case. This spatial resolution value corresponds to a capacitance resolution of 108.5 fF (that is about -77 dB). A suitable ADC [18] has been utilized for better reading of the output voltage.

A comparison of the main characteristics of the presented interfaces, with respect to those reported in the literature, is here presented in Table 1. We underline the fact that the works reported in [6, 10] are related to a single ended capacitive sensor (despite the second one is showing a differential output and its approach is also applicable to ratiometric sensors). The here proposed circuits show better values of sensitivity and resolution (in dB), also being constant for each operating point.

Table 1

Ref. number	Application	Approach	Type of conversion	Technology	Measurable capacitance features	Accuracy (error)	Sensitivity	Resolution
[2]	Micro-accelerometers	VM	switched-capacitor (A/D conversion)	Integrated	Csens > 80 pF	n.a.	0.26–1.6 V/g	1.6 $\mu\text{g}/\text{Hz}$
[5]	MEMS	VM	switched-capacitor (A/D conversion)	Discrete	$C_0 = 500 \text{ pF}$ ($C_1 = C_2 = 250 \text{ pF}$) Range $\pm 50\%$	$\pm 0.03\%$	n.a.	at least 10 pF (–34 dB)
[6]	Grounded capacitive sensors	VM	C to Period (A/D conversion)	Integrated 0.7 μm CMOS	$C_0 = 100 \text{ pF}$ –2 μF Range $\pm 50\%$	Non-linearity error = 0.2%	n.a.	n.a.
[7]	MEMS	VM	C to Phase	Integrated 0.35 μm CMOS	$C_0 = 10 \text{ pF}$ Range $\pm 50\%$	$\pm 0.02\%$	n.a.	n.a.
[8]	Differential capacitive sensors	VM	C to Period (A/D conversion)	Discrete	$C_0 = 400 \text{ pF}$ ($C_1 = C_2 = 200 \text{ pF}$) Range $\pm 50\%$	$\pm 0.2\%$	n.a.	10 pF (–32 dB)
[9]	Accelerometers	VM	C to V	Discrete	$C_0 = 20 \text{ pF}$ Range $\pm 120\%$	$\Delta V = 1.5 \text{ mV}$	0.1 mV/fF	20 fF (–60 dB)
[10]	Capacitive/resistive sensors	VM	C to V	Integrated 0.8 μm CMOS	$C_0 = 1 \text{ pF}$ Range $\pm 75\%$	Non-linearity error = 1%	n.a.	1.13 fF (–59 dB)
[11]	Biomimetic hair flow sensors	VM	C to V	Integrated 0.35 μm CMOS	$C_0 = 25 \text{ pF}$ Range $\pm 30\%$	0.5–3.4%	6–21 mV/ μm	23–83 nm (from –77 to –65 dB)
This work 1st sol.	Differential capacitive sensors	CM	C to V	Discrete	$C_0 = 800 \text{ pF}$ ($C_1 = C_2 = 400 \text{ pF}$) Range $\pm 10\%$	0.01–0.09%	constant 8.54 V/ μm	674 pm 89.85 fF (–79 dB)
This work 2nd sol.	Differential capacitive sensors	CM	C to V	Discrete	$C_0 = 800 \text{ pF}$ ($C_1 = C_2 = 400 \text{ pF}$) Range $\pm 10\%$	< 0.2% (simul.) < 3.2% (meas.)	constant 8.13 V/ μm	814 pm 108.5 fF (–77 dB)

Note: VM = Voltage mode; CM = Current mode

4 Conclusions

We have shown two novel current-mode analog interfaces for revealing and measuring ratiometric capacitive sensors. Experimental measurements have been performed on a discrete element board, employed through a commercial CCII (AD844). Both of our proposed architectures have shown a good agreement with the theoretical expectations. Sensitivity and resolution (showing constant values for each considered working point) have been determined in a practical case, showing satisfactory values.

References

1. L.K. Baxter, *Capacitive sensors: design and applications*, vol. 1 (John Wiley & Sons, New York, 1996)
2. N. Yazdi, H. Kulah, K. Najafi, Precision readout circuits for capacitive microaccelerometers. *Proc. IEEE Sens.* 24–27 (2004)
3. M.N. Horenstein, J.A. Perreault, T.G. Bifano, Differential capacitive position sensor for planar MEMS structures with vertical motion. *Sens. Actuators* **80**, 53–61 (2000)
4. R.E. Oosterbroek, T.S.J. Limmerink, J.W. Berenshot, G.J.M. Krijnen, M.C. Elwenspoek, A. van den Berg, A micromachined pressure/flow-sensor. *Sens. Actuators* **77**, 167–177 (1999)
5. B. George, V.J. Kumar, Switched capacitor signal conditioning for differential capacitive sensors. *IEEE Trans. Instrum. Measur.* **56**, 913–917 (2007)
6. Q. Jia, G. Meijer, X. Li, C. Guan, An integrated interface for grounded capacitive sensors, in *Proceedings of the 4th IEEE Sensors Conference*. Irvine. Oct 2005, pp. 4–5
7. T.G. Constandinou, J. Georgiou, C. Toumazou, A micropower front-end interface for differential-capacitive sensor systems, in *Proceedings of the IEEE International Symposium on Circuits and Systems*. Seattle. May 2008, pp. 2474–2477
8. N.M. Mohan, A.R. Shet, S. Kedarnath, V.J. Kumar, Digital converter for differential capacitive sensors. *IEEE Trans. Instrum. Meas.* **57**, 2576–2581 (2008)
9. K. Mochizuki, K. Watanabe, T. Masuda, A high-accuracy high-speed signal processing circuit of differential-capacitance transducers. *IEEE Trans. Instrum. Meas.* **47**, 1244–1247 (1998)
10. T. Singh, T. Sæther, T. Ytterdal, Current-mode capacitive sensor interface circuit with single-ended to differential output capability. *IEEE Trans. Instrum. Meas.* **58**, 3914–3920 (2009)
11. G. Ferri, F.R. Parente, V. Stornelli, G. Pennazza, M. Santonico, A. D’Amico, A standard CMOS technology fully-analog differential capacitance sensor front-end, in *Proceedings of the International Workshop on Advanced Sensor Interface*. Gallipoli. June 2015, pp. 152–157
12. G. Ferri, N.C. Guerrini, *Low-voltage low-power CMOS current-conveyors* (Kluwer Academic Publisher, Boston, 2003)
13. G. Ferri, A. De Marcellis, C. Di Carlo, V. Stornelli, A. Flammini, A. Depari, D. Marioli, E. Sisinni, A CCII-based low-voltage low-power read-out circuit for DC-excited resistive gas sensors. *IEEE Sens. J.* **9**, 2035–2041 (2009)
14. G. Ferri, V. Stornelli, A. di Simone, A CCII-based high impedance input stage for biomedical applications. *J. Circuits Syst. Comput.* **20**(8), 1441–1447 (2011)
15. V. Stornelli, G. Ferri, A 0.18 μm CMOS DDCCII for portable LV-LP filters. *Radioengineering* **22**(2), 434–439 (2013)

16. C. Falconi, G. Ferri, V. Stornelli, A. De Marcellis, D. Mazziari, A. D'Amico, Current-mode high-accuracy high-precision CMOS amplifiers. *IEEE Trans. Circuits Syst. II* **55**(5), 394–398 (2008)
17. A. De Marcellis, G. Ferri, *Analog Circuits and Systems for Voltage-Mode and Current-Mode Sensor Interfacing Applications* (Springer, 2011)
18. G. Bonfini, A.S. Brogna, C. Garbossa, L. Colombini, M. Bacci, S. Chicca, F. Bigongiari, N. C. Guerrini, G. Ferri, An ultra low power switched opamp-based 10-bit integrated ADC for implantable biomedical applications. *IEEE Trans. Circuits Syst.* **51**, 174–177 (2004)